

Influence of hydrodynamics on many-particle diffusion in 2D colloidal suspensions

E. Falck^{1,2,a}, J.M. Lahtinen¹, I. Vattulainen^{1,2}, and T. Ala-Nissila^{1,3}

¹ Laboratory of Physics - Helsinki University of Technology, P.O. Box 1100, FIN-02015 HUT, Finland

² Helsinki Institute of Physics - Helsinki University of Technology, P.O. Box 1100, FIN-02015 HUT, Finland

³ Department of Physics - Box 1843, Brown University, Providence RI 02912-1843, USA

Received 20 February 2003 and Received in final form 20 October 2003 /

Published online: 23 March 2004 – © EDP Sciences / Società Italiana di Fisica / Springer-Verlag 2004

Abstract. We study many-particle diffusion in 2D colloidal suspensions with full hydrodynamic interactions through a novel mesoscopic simulation technique. We focus on the behaviour of the effective scaled tracer and collective-diffusion coefficients $D_T(\rho)/D_0$ and $D_C(\rho)/D_0$, respectively, where D_0 is the single-particle diffusion coefficient, as a function of the density of the colloids ρ . At low Schmidt numbers $Sc \sim 1$, we find that hydrodynamics has essentially no effect on the behaviour of $D_T(\rho)/D_0$. At larger Sc , $D_T(\rho)/D_0$ seems to be enhanced at all densities, although the differences compared to the case without hydrodynamics are rather minor. The collective-diffusion coefficient, on the other hand, is much more strongly coupled to hydrodynamical conservation laws and is distinctly different from the purely dissipative case without hydrodynamic interactions.

PACS. 68.35.Fx Diffusion; interface formation – 05.40.-a Fluctuation phenomena, random processes, noise, and Brownian motion – 82.20.Wt Physical chemistry and chemical physics: Computational modeling; simulation

1 Introduction

The dynamics of Brownian particles in confined geometries, and in two dimensions (2D) in particular, is an important theoretical problem with applications in surface science and colloidal systems [1–3]. Examples of fundamental questions that have been addressed recently are the form of effective interactions between macroions in a colloidal suspension [4, 5] and the effects of hydrodynamic interactions (HIs) on the diffusive properties of colloidal particles [6–10].

So far, most studies have focused on *self-diffusion* of particles in 2D. In the ideal case of no external potential and without HIs, the density-dependent self-diffusion coefficients of 2D hard-disk particles have been recently determined using numerical simulations [11, 12] and various theoretical approximations [12–15]. While the single-particle limit in the ideal case is trivial, no exact analytic results exist for finite densities. In this regime complicated many-body effects manifest themselves through memory effects in the motion of tagged colloidal particles.

The situation is even more complicated when the HIs mediated by the solvent in a colloidal suspension are taken into account. Recent work on the self-diffusion of colloidal

particles in 2D and quasi-2D [6–10] indicates that HIs do indeed influence self-diffusion. For hard spheres, HIs have been shown to slow down self-diffusion [8]. The case is more subtle in systems where interactions are softer and relatively long-ranged, since then self-diffusion appears to be enhanced [6–10]. Hence, the nature and magnitude of these subtle effects in a given system depend on the relative importance of hydrodynamic and other interactions.

While the self-diffusion properties of 2D colloidal systems are relatively well understood, much less is known about *collective diffusion* in 2D colloidal suspensions. Nevertheless, collective diffusion plays a crucial role in processes such as spreading and phase separation, as it describes the decay rate of density fluctuations in a system. While the case without HIs has been considered recently [12, 16], the theoretical understanding of 2D situations with HIs is surprisingly limited. This is, in part, due to theoretical difficulties when dealing with collective transport in 2D liquids with full hydrodynamics. Furthermore, realistic numerical simulations of collective diffusion in hydrodynamic two-phase colloidal systems have turned out to be a considerable methodological challenge.

In this paper, our purpose is to employ a recently proposed mesoscopic simulation method [17–19] to shed light on some of the fundamental issues of many-particle diffusion in 2D colloids. To this end, we consider an ensemble

^a e-mail: efalck@cc.hut.fi

of colloidal particles that interact mutually with a short-range repulsive potential and long-range HIs. The importance of HIs in the present case is quantified through a comparison to a previous study [12] in which HIs were neglected altogether.

The main issue we want to address here is the influence of hydrodynamics on the diffusive dynamics of this system. We study tracer and collective diffusion for a wide range of colloid concentrations. Our study reveals that the tracer and collective diffusion of colloids in the present model suspension are distinctly different in nature. While the influence of hydrodynamics on tracer diffusion is relatively weak, the collective diffusion is much more strongly coupled to hydrodynamics. When previous results without hydrodynamics [12] are compared to the present results with HIs, we can conclude that the concentration dependence of collective diffusion changes completely.

2 Schmidt number

An important quantity measuring the properties of a fluid in equilibrium is the dimensionless Schmidt number Sc , defined as the ratio of momentum diffusivity to mass diffusivity:

$$Sc = \frac{\nu}{D}. \quad (1)$$

Here $\nu = \eta/\rho_s$ is the kinematic viscosity of the fluid, η being the viscosity and ρ_s the density of the fluid, and D is the tracer diffusion coefficient of the fluid particles.

In a real fluid such as water $Sc \sim 10^3$. Theoretical arguments, too, often include the assumption that hydrodynamic fluctuations have reached a steady state on the time scale of the motion of the colloidal particles. The situation can be quite different in computer simulations: efficient mesoscopic simulation techniques such as dissipative particle dynamics (DPD) typically have $Sc \sim 1$ [20] due to soft interactions often used in DPD simulations. Larger Schmidt numbers could be obtained by using hard conservative interactions, but then the benefits of DPD would, for the most part, be lost. Other mesoscopic simulation techniques such as the Lowe-Andersen method [21] permit a wider range of Schmidt numbers even in the case of soft interactions, but the numerical load of updating the positions and velocities of all solvent and solute particles remains formidable. This is particularly problematic in dilute solutions where an individual macromolecule is embedded in a solvent. Here the computational cost is mainly due to the solvent degrees of freedom, and only a small fraction of the computing time is spent on the macromolecule of interest.

Overall, for low Schmidt numbers, the hydrodynamic interactions are still developing on the time scale at which the colloids are diffusing, and hence the dynamics of the colloids and the fluid velocity field are coupled. The actual effect on the dynamics of the colloids can in this case be very complicated, and is not fully understood. Clearly, there is a need for efficient techniques that can be used for modelling systems with hydrodynamic interactions under

a variety of conditions, including both dilute and concentrated solutions, and cases where Sc is varied in a controlled fashion. The method discussed below is a promising attempt in this direction.

3 Simulation method

The model system we consider comprises an ensemble of disks immersed in a 2D liquid. The dynamics of the system is simulated using a novel mesoscopic technique introduced by Malevanets and Kapral (MK) [17,18]. The MK method is a hybrid molecular-dynamics (MD) model, where the colloid is treated microscopically, and the solvent obeys coarse-grained dynamics. Despite the fact that it has been introduced recently, the MK method has been applied to a number of interesting problems, including studies of dilute polymer systems [22], molecular clusters [23], individual colloids under flow [18] and flow around a cylinder in a 2D channel [24]. A variant of the MK method by Malevanets and Yeomans has been applied to binary fluid mixtures [25] and structural and dynamical properties of individual polymer chains in a hydrodynamic medium [19,26]. The methodology of the technique has further been developed and discussed in references [27–30].

Let us first concentrate on the coarse-grained solvent. The solvent consists of N_s particles of mass m_s with continuous positions and velocities. The dynamics of these solvent particles consists of free streaming interrupted by multi-particle collision events. The time is partitioned into segments (collision steps) τ , and the system itself is divided into cells (collision volumes). The simplest tessellation is a square grid with a mesh size a . During streaming, the position of the particle i changes as follows:

$$\mathbf{x}_i(t + \tau) = \mathbf{x}_i(t) + \tau \mathbf{v}_i(t). \quad (2)$$

Here \mathbf{v}_i is the velocity of the particle i . Collisions, in turn, involve the exchange of momentum among the solvent particles in a given cell. In practice, the velocities of the particles are transformed as

$$\mathbf{v}_i(t + \tau) = \mathbf{V} + \boldsymbol{\omega} \cdot [\mathbf{v}_i(t) - \mathbf{V}], \quad (3)$$

where \mathbf{V} is the average velocity of all the particles in the cell the particle i belongs to and $\boldsymbol{\omega}$ is a random rotation matrix chosen separately for each cell. It can be shown [17] that this dynamics consisting of a superposition of streaming and collision events conserves the momentum and energy in each collision volume, and gives a correct description of the hydrodynamics of the velocity field. Illuminating pictures of steady-state flow fields in various geometries can be found, *e.g.*, in reference [17]. Note that the technique does not, however, give a correct description of the dynamics at microscopic time scales [18].

The coarse-grained collision dynamics can be combined with a full molecular-dynamics description of embedded solute molecules in the solvent. Such an approach is very convenient if it is sufficient to account for the influence of the explicit solvent on the solute dynamics, without paying attention to the microscopic details of the solvent. The solvent-colloid and colloid-colloid interactions

V_{sc} and V_{cc} , respectively, can be chosen as in MD, while the interaction potential between two solvent particles is always zero. Within time segments of length τ , the system is evolved by Newton's equations of motion:

$$\frac{\partial \mathbf{x}_i(t)}{\partial t} = \mathbf{v}_i(t), \quad (4)$$

$$m_i \frac{\partial \mathbf{v}_i(t)}{\partial t} = -\frac{\partial V}{\partial \mathbf{x}_i}. \quad (5)$$

Here m_i is the mass of particle i and $V = V_{cc} + V_{sc}$. As $V_{ss} = 0$, solvent molecules will undergo free streaming unless they interact with a colloid. The effective solvent-solvent interactions take place as multi-particle collisions at intervals of τ : the velocities of the solvent particles are transformed according to equation (3).

The MK method reduces computing times significantly compared to ordinary MD simulations for colloidal systems, especially in the case of dilute macromolecular solutions. An even faster variant of the MK algorithm has been introduced by Malevanets and Yeomans in reference [19]. In this case also the direct solvent-colloid interaction is absent, and the solvent-colloid interaction is described indirectly through collisions. Another variation has been suggested by Ihle *et al.* in reference [28]. They pointed out that if the distance the solvent particles travel between the collisions (the mean free path) is small compared to the linear size of the collision volume, there will be unphysical correlations at short time and length scales. To mend this problem, they suggested a random shift of the grid of collision volumes. In practice, all solvent particles are shifted by the same random vector before a collision. After the collision, the particles are shifted back by the same vector. This procedure will ensure that particles in a given cell will not remain correlated over several collision steps.

When designing an MK simulation, one has to pay attention to a number of important details. The parameters that determine the collision dynamics—the mesh size, the collision step, and the rotation operator—determine the properties of the coarse-grained solvent, *e.g.*, the solvent viscosity and the Schmidt number. Hence, one should select these parameters carefully. However, in selecting the parameters a number of constraints must be taken into account.

When selecting the mesh size a for the collision volumes, one should, for the sake of efficiency, ensure that there are enough solvent particles in a cell. The cells, however, cannot be arbitrarily large: in that case the local conservation breaks down. In addition, if the cells are very large compared to the mean free path, there will be correlations at short time and length scales. Hence, the solvent density and the average velocity of the solvent particles (*i.e.* the temperature) influence the choice of a . Additionally, when colloids are embedded in the solvent, the mesh size a should be chosen such that several colloid molecules cannot be present in the same collision volume. In particular, if the direct solvent-colloid interactions are replaced by collisions, several colloid molecules in the same cell could lead to problems.

The choice of the rotation operator is another issue. A convenient choice is to perform rotations about a vector which has been chosen uniformly from the surface of a unit sphere. The rotation angles may, *e.g.*, be chosen such that either an angle $+\alpha$ or $-\alpha$ is chosen with probability $1/2$. The collision step τ , in turn, should be long enough to provide a sufficiently long mean free path. On the other hand, τ should be chosen small enough to incorporate correctly the effect of solvent dynamics on the colloids.

The above-mentioned choices are not independent: if one, *e.g.*, alters a , the solvent viscosity is affected, and one might have to reconsider the choice of τ to make sure that there will be correct hydrodynamic interactions between the colloid particles. Hence, it can be quite challenging to obtain the desired transport properties for the fluid, *e.g.* the Schmidt number, and fulfil all constraints at the same time: in some cases one has to compromise. In most cases, several parameters need to be changed simultaneously. In this work, we have paid particular attention to account for all of these points. In the following section, we will elaborate on our choices of parameters.

4 Model system

The direct interactions between the colloid particles are strongly repulsive and of short range. The interaction potentials are of the form

$$V_{kl}(r) = \begin{cases} \epsilon_{kl} \left(\frac{\sigma_{kl}}{r}\right)^n, & r \leq r_c \equiv 2.5\sigma; \\ 0, & r > r_c, \end{cases} \quad (6)$$

where r is the separation between two particles of type k and l ($k, l \in \{c, s\}$). Here we set $n = 12$, which allows a direct comparison with previous calculations on a smooth surface without hydrodynamics [12]. The colloid-colloid interaction parameters are $\sigma_{cc} = 2\sigma$ and $\epsilon_{cc} = \epsilon$, while the solvent-colloid ones are $\sigma_{cs} = \sigma$ and $\epsilon_{cs} = \epsilon$ or zero, *i.e.* in some cases there is no direct solvent-colloid interaction, see above. The colloidal particles have a mass $m_c = 5m$, and the solvent mass is set to $m_s = m$ or $m_s = 0.5m$. Note that the description considered here is coarse grained rather than molecular. Thus, the solvent particles discussed here should be considered as coarse-grained particles representing clusters of solvent molecules, and therefore the mass and size ratios of colloid and solvent particles do not represent those of the actual molecules (for further discussion, see Ref. [17]).

The parameters σ , ϵ and m now define our system of units, and hence our unit of time is given by $\tau_{LJ} = \sigma(m/\epsilon)^{1/2}$. The temperature is $k_B T = 2\epsilon$, and for the dimensionless solvent density we use $\rho_s = 1$. The dimensionless solvent and colloidal densities have been defined as $\rho_s \equiv N_s/(A/\sigma_{cs}^2)$ and $\rho \equiv N/(A/\sigma_{cc}^2)$, respectively. Here A is the area of the system, N_s the number of solvent particles and N the number of colloidal particles. In these units, the density of a closed-packed colloidal system is $\rho \approx 1.15$. The equations of motion were integrated using the velocity Verlet algorithm with a time step $\delta t = 0.005\tau_{LJ}$, and periodic boundary conditions were employed in all directions.

Table 1. A summary of the three different parameter sets used. See text for details.

Sc	$\nu [\sigma^2 \tau_{LJ}^{-1}]$	$\tau [\tau_{LJ}]$	$a [\sigma]$	α	$m_s [m]$	$L [\sigma]$
1	0.82(1)	0.5	2	$\pm 90^\circ$	1	200
20	3.70(2)	0.05	2	$\pm 125^\circ$	0.5	100
100	9.11(2)	0.1	2	$\pm 170^\circ$	1	100

As mentioned in the previous section, the parameters that determine the collision dynamics should be chosen very carefully. In this study our aim is to fulfil the constraints discussed above as well as possible, and additionally to control the Schmidt number Sc . The value of Sc is influenced, *e.g.*, by the choice of the collision step τ , the grid size a , the rotation angle α and the solvent mass m_s . We have used different sets of parameters in the simulations. These sets have been tuned to yield different kinematic viscosities and Schmidt numbers. As Ihle *et al.* point out in reference [28], one should, by varying the mean free path and rotation angle α , be able to simulate fluid with a wide range of Schmidt numbers. Note that one thus, to achieve a perceptible change in the Schmidt number, has to accept that quite a few parameters must be reset, and also that all changes could affect the constraints mentioned above. Embedding solvent molecules into the solvent increases the number of constraints and tends to complicate matters.

A list of the three different parameter sets and the resulting relevant solvent properties is shown in Table 1. The kinematic viscosities ν in Table 1 were computed using equations (4–6) in reference [28], and the Schmidt numbers were obtained from equation (1). The diffusion coefficients for the solvent molecules were computed using the memory expansion method from reference [31]. The memory expansion method, as shown in reference [31], yields results entirely consistent with the more traditional mean-square displacement analysis, while it is computationally considerably more efficient.

Let us now briefly assess the choice of parameters from the point of view of the constraints discussed above. As for the grid size a , it has been set to 2σ in all systems. Recalling that $\sigma_{cc} = 2\sigma$, we can be assured that there is at most one colloid in each cell. As the solvent density $\rho_s = 1$, there are on the average four solvent molecules in each cell. This is perhaps not optimal, but reasonably efficient. The collision time τ has been assigned a value of either $0.5\tau_{LJ}$ or $0.1\tau_{LJ}$. This means that the systems with $Sc > 1$ have a mean free path (distance travelled during τ) of the order of $0.1a$. In these cases, to avoid unphysical correlations at short time and length scales, we have employed the random grid-shifting procedure proposed in reference [28]. The hydrodynamics, in turn, is adequately described at time scales that are at least an order of magnitude larger than the collision time τ . Recalling that the kinematic viscosity ν describes the diffusivity of momentum, we can conclude that the length scales beyond which the hydrodynamics should be valid are of the order of the diameter of the colloidal particles σ_{cc} .

5 Results

5.1 Tracer diffusion

Perhaps the most well-known transport coefficient is the tracer diffusion coefficient D_T , which describes the motion of a tagged tracer particle as $D_T = \lim_{t \rightarrow \infty} D_T(t)$, where the time-dependent transport coefficient $D_T(t)$ is given by the Green-Kubo description

$$D_T(t) = \frac{1}{dN} \sum_{i=1}^N \int_0^t dt' \langle \mathbf{v}_i(t') \cdot \mathbf{v}_i(0) \rangle \quad (7)$$

among N identical particles. Here $d = 2$ is the dimensionality of the system and $\mathbf{v}_i(t)$ is the velocity of particle i at time t . The quantity $\phi(t) \equiv \langle \mathbf{v}_i(t) \cdot \mathbf{v}_i(0) \rangle$ is the velocity autocorrelation function. Alternatively, it is common to define the tracer diffusion coefficient through the mean-square displacement

$$\langle [\mathbf{r}(t)]^2 \rangle \equiv \frac{1}{2dN} \sum_{i=1}^N \langle [\mathbf{r}_i(t) - \mathbf{r}_i(0)]^2 \rangle, \quad (8)$$

but in that case the definition of the time-dependent counterpart would be less convenient. Hence, in this study, we determined $D_T(t)$ through equation (7) using the memory expansion technique discussed in references [31, 32].

Equation (7) expresses the fact that we are dealing with a time-dependent quantity $D_T(t)$. Since this is also the case in experiments, let us briefly discuss why it is important to consider diffusion coefficients in 2D and quasi-2D cases as time-dependent ones.

For colloidal systems with HIs, it has been known since the 1970s that there are long-time tails in the velocity autocorrelation functions. These have been observed in MD [33] and lattice-Boltzmann [34] simulations, and lead to a divergence of the tracer diffusion coefficient in 2D [33, 35–37]. In this case, the diffusion coefficients $D_T(t)$ have to be considered as time-dependent, effective quantities. This matter is not just a theoretical issue, but concerns both computational and experimental approaches.

When tracer diffusion in concentrated suspensions is investigated experimentally, it is common to single out the effects of the HIs by concentrating on the so-called short-time diffusion coefficients [6, 7, 10, 38]. These are measured at times much shorter than τ_I , the time it takes the tracer particles to diffuse the average distance between the suspended colloidal particles. For this definition to be meaningful, such times should be significantly larger than the time τ_B it takes for the velocities of the colloidal particles to relax. In our case, for concentrated solutions and small values of Sc in particular, the time interval between τ_B and τ_I becomes very narrow. Furthermore, as the MK method has been developed for studies in the hydrodynamic regime, we cannot expect that it generates the correct dynamics at very short (microscopic) time and length scales. Hence, this definition for short-time diffusion coefficients is not appropriate for the present study.

In this work, we consider $D_T(\rho, t)$ normalised by the single-particle diffusion coefficient $D_0(t) \equiv D_T(\rho \rightarrow 0, t)$.

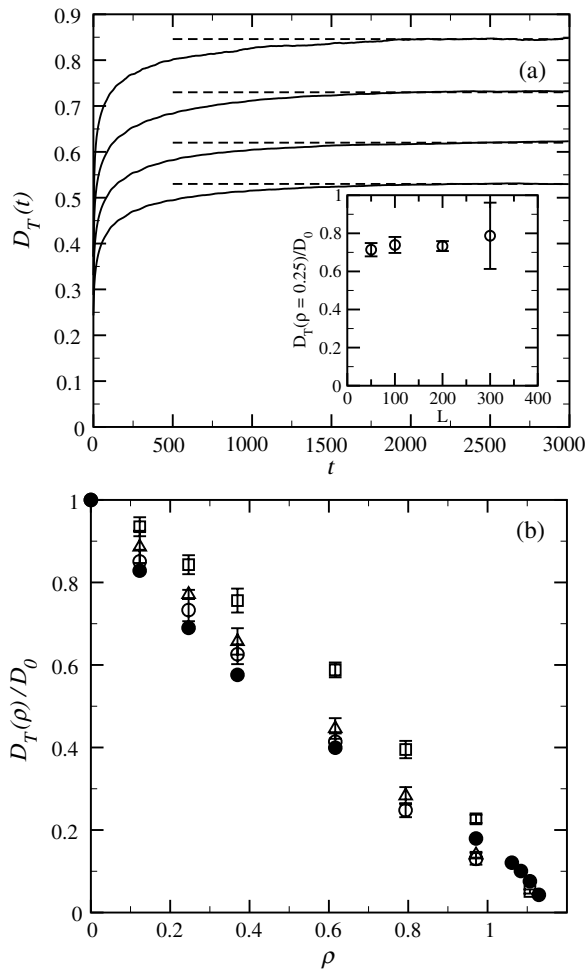


Fig. 1. (a) Tracer diffusion coefficients $D_T(\rho, t)$ as a function of t for $Sc \approx 1$. These data have been obtained from simulations without solvent-colloid interactions. The colloidal densities from top to bottom are 0, 0.1232, 0.2464 and 0.3697, and the dashed lines highlight the plateaus from which the effective diffusion coefficients have been determined. The inset shows the effective scaled diffusion coefficient $D_T(\rho)/D_0$ at $\rho = 0.2464$ as a function of the system size L . (b) Effective scaled tracer diffusion coefficients $D_T(\rho)/D_0$ as a function of ρ for $Sc \approx 1$ (open circles), $Sc \approx 20$ (open triangles) and $Sc \approx 100$ (open boxes). For reference, results without HIs [12] are also presented (solid circles).

As shown in Figure 1(a), within the accuracy of the data, the tracer diffusion coefficients $D_T(\rho, t)$ converge to a finite limit in the limit of long times. Although the slow logarithmic divergences are present in our data (data not shown), the amplitudes of the tails at late simulation times are exceedingly small and partially masked by statistical fluctuations. Hence, effective values $D_T(\rho)$ for the tracer diffusion coefficients can be extracted from the plateau region. In the dilute limit, the plateau region yields the effective single-particle diffusion coefficient D_0 . The effective scaled diffusion coefficients are then defined as $D_T(\rho)/D_0$.

The possible finite-size effects on the measured scaled diffusion coefficients were also examined. In the inset of

Figure 1(a), we show the scaled tracer diffusion coefficient $D_T(\rho)/D_0$ at the density $\rho = 0.2464$ for the case $Sc \approx 1$ as a function of the system size. Since both $D_T(\rho)$ and D_0 have a similar system size dependence, our results suggest that the scaled quantity does not depend in any significant manner on the system size used in the simulations.

In Figure 1(b) we show a summary of our results for the scaled $D_T(\rho)/D_0$ as a function of the dimensionless density of the disks ρ . For comparison we also present our earlier Brownian dynamics (BD) results for the purely dissipative case [12]. As stated in reference [12], in purely dissipative systems, where the interaction potential is of the form in equation (6), the results can be made consistent with hard-disk results by a simple scaling of the density. Through the scaling

$$\tilde{\rho} = \left(\frac{\epsilon}{k_B T} \right)^{2/n} \rho, \quad (9)$$

where $\tilde{\rho}$ is the corresponding dimensionless density in the hard-disk system, we can transform the hard-disk data presented in reference [12] such that they correspond to the interaction potential and temperature used in the present study.

It is clear that at low values of Sc hydrodynamics has virtually no effect on tracer diffusion. As Sc is tuned to larger values, we find a minor *enhancement* of $D_T(\rho)/D_0$, which is largest at intermediate densities $\rho \approx 0.4-0.7$. Thus, the hydrodynamics does not give rise to major deviations from the case without HIs. Further, in the concentrated regime the tracer diffusion is considerably slowed down compared to the dilute limit, and slightly beyond $\rho = 1$ the tracer diffusion is essentially frozen due to packing constraints. Yet the phase behaviour in this limit was found to be fluid-like, *i.e.*, we did not observe transitions to ordered phases. We conclude that HIs do play a role here, but their influence on the scaled tracer diffusion coefficient seems to be rather minor.

5.2 Collective diffusion

An important transport coefficient characterising the decay rate of *collective* density fluctuations is the collective-diffusion coefficient D_C , which should not be confused with the tracer diffusion coefficient D_T describing the motion of a *tagged tracer particle* as defined above by equation (7). The collective-diffusion coefficient can be written as $D_C = \lim_{t \rightarrow \infty} D_C(t)$, where $D_C(t)$ is now defined through the Green-Kubo relation

$$D_C(t) = \xi D_{cm}(t) = \xi \frac{1}{dN} \int_0^t dt' \langle \mathbf{J}(t') \cdot \mathbf{J}(0) \rangle. \quad (10)$$

Here $\xi = \langle N \rangle / [\langle N^2 \rangle - \langle N \rangle^2]$ is the thermodynamic factor inversely proportional to the isothermal compressibility, and $\mathbf{J}(t) = \sum_{i=1}^N \mathbf{v}_i(t)$ is the total particle flux. Note that the autocorrelation function $\langle \mathbf{J}(t) \cdot \mathbf{J}(0) \rangle$ is not a single-particle quantity, but must be computed over the velocities of *all* N particles. Consequently, the term $D_{cm}(t)$ can

be interpreted as the time-dependent diffusion coefficient characterising the center-of-mass (CM) motion of the N particles under study. Following the approach discussed above for tracer diffusion, one could approach the same idea in terms of the mean-square displacement

$$\langle[\mathbf{R}_{\text{cm}}(t)]^2\rangle \equiv \frac{1}{2dNt} \langle[\mathbf{R}(t) - \mathbf{R}(0)]^2\rangle, \quad (11)$$

where $\mathbf{R}(t) = \sum_{i=1}^N [\mathbf{r}_i(t) - \mathbf{r}_i(0)]$ is the CM position of the N particles at time t [39]. As in the case of tracer diffusion, however, it is less convenient to define $D_{\text{cm}}(t)$ in this fashion. Thus, we have focused on equation (10) and used the memory expansion technique.

The thermodynamic factor ξ , which is a static quantity, is not affected by hydrodynamics within our accuracy. To estimate ξ we have used data from our MK simulations and the so-called Boublik approximation [40]. These are in excellent agreement as demonstrated by the inset of Figure 2(a) and reference [12].

In the case of dissipative hard spheres on a smooth surface, there is an exact result that the CM mobility D_{cm} is independent of the density ρ [13]. This is because the interparticle interactions preserve the CM momentum, and thus $D_{\text{cm}}(\rho) = D_{\text{cm}}(0) = \text{const}$. However, with HIs in place this argument no longer holds. In Figure 2(a) we show the scaled CM mobility as a function of density in the present system. Note that the effective scaled CM mobilities $D_{\text{cm}}(\rho)/D_0$ have been determined in the same manner as the effective scaled self-diffusion coefficients $D_{\text{T}}(\rho)/D_0$. Now, we find that the scaled CM mobility is a decreasing function of ρ , and decreases much more rapidly than $D_{\text{T}}(\rho)/D_0$ shown in Figure 1(b). It should also be noted that $D_{\text{cm}}(\rho)/D_0$ does not appear to be sensitive to Sc : while the self-diffusion of individual particles is slightly influenced by Sc , the effects on individual particles seem to be largely independent of each other, and thus cancel out in the CM mobility.

In Figure 2(b) we show the scaled collective-diffusion coefficient that displays a slight *minimum* or a plateau at small values of the density ρ . The source of the interesting shape is the interplay of ξ and $D_{\text{cm}}(\rho)/D_0$: although the thermodynamic factor increases monotonously, the initial decay of the scaled CM diffusion coefficient is much more rapid and dominates the behaviour of the scaled collective-diffusion coefficient at small concentrations. The crossover takes place around $\rho \approx 0.2$ – 0.3 , above which the behaviour of the scaled collective-diffusion coefficient is dictated by the thermodynamic factor. A comparison with Figure 1(b) shows that the tracer and collective-diffusion coefficients are essentially identical up to this crossover concentration. In the dilute limit this is expected, since then $D_{\text{C}} = D_{\text{T}}$. At concentrations above $\rho \approx 0.2$ this consistency breaks down due to particle number fluctuations that at large concentrations govern collective diffusion in the present system, and give rise to a scaled collective-diffusion coefficient whose behaviour is completely different from its tracer counterpart.

From our data we can conclude that the HIs have a significant effect on collective diffusion. Figure 2(b) shows

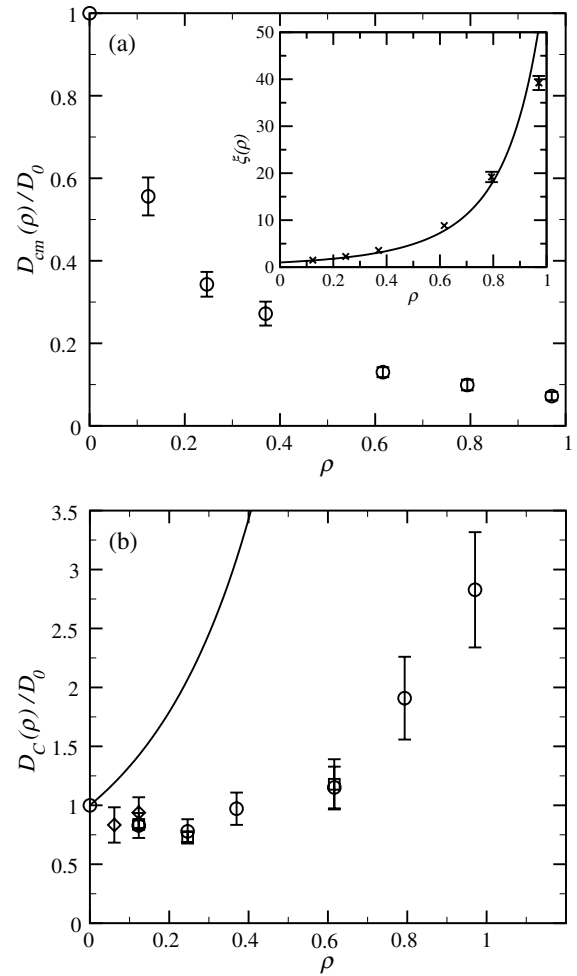


Fig. 2. (a) Scaled CM mobility $D_{\text{cm}}(\rho)/D_0$ as a function of ρ for $Sc \approx 1$. The inset shows the thermodynamic factor ξ from the Boublik approximation [40] (solid line) and from our simulations (crosses). (b) Effective scaled collective-diffusion coefficients $D_{\text{C}}(\rho)/D_0$ as a function of ρ . Open circles are results with $Sc \approx 1$, obtained from simulations without solvent-colloid interactions. Open diamonds are results from simulations where the solvent-colloid interactions are present. Squares, in turn, are from computations where $Sc \approx 100$. For reference, the solid line is $D_{\text{C}}(\rho)/D_0$ in the case where HIs have not been taken into account [12].

that the behaviour of $D_{\text{C}}(\rho)/D_0$ is in striking contrast to the dissipative case (without HIs) which is entirely determined by ξ . We argue that this behaviour is generic in colloidal suspensions governed by hydrodynamics, since then the CM mobility is not constant, but competes with ξ . The actual form of $D_{\text{C}}(\rho)/D_0$, however, may vary from one system to another, depending on the details of interactions and the impact of the HIs. Further studies, experiments in particular, are called for.

5.3 Role of dynamics

Most of the data we have presented in this study, see Figures 1 and 2, have their origin in MK simulations where

the conventional solvent-colloid interactions have been replaced by the colloid particles participating in the multi-particle collisions. Including explicit solvent-colloid interactions into the simulations is, of course, straight-forward, but the computational cost then increases considerably compared to simulations without explicit solvent-colloid interactions. This point is particularly important in studies of collective diffusion, in which case the computational effort is extensive.

To make sure that the minimum seen in $D_C(\rho)/D_0$ *vs.* ρ in Figure 2(b) is not an artefact generated by the omission of the conventional solvent-colloid interactions, we computed for a few densities ($\rho \leq 0.2$) the effective scaled diffusion coefficients with the conventional solvent-colloid interactions in place.

We first found that the absolute, unscaled diffusion coefficients calculated with and without explicit solvent-colloid interactions differ slightly. This is expected, since the effective friction between the solvent and the colloids is altered when the direct solvent-colloid interactions are left out. Based on our simulations for the present model, the effect is similar for all concentrations. Hence, if we scale the diffusion coefficients by the single-particle diffusion coefficient, the scaled diffusion coefficients are, within our numerical accuracy, unaltered, when the dynamics is varied. This result is illustrated in Figure 3.

The key finding is that when we consider the low-density regime for the scaled collective-diffusion coefficient, both schemes, *i.e.* the cases with and without direct solvent-colloid interactions, yield the same behaviour with the minimum or plateau $D_C(\rho)/D_0 \approx 0.75$ close to $\rho \approx 0.2-0.3$ (see Fig. 2(b)). Thus, we are confident that the behaviour observed here for collective diffusion is a true finding and not merely due to the dynamics used in this study. This conclusion is further supported by very recent mode-coupling calculations [41] that have predicted a behaviour similar to what we have observed in this work, including a minimum at intermediate densities. The minimum seems to be very robust: it is found for a wide range of parameter values [41].

6 Discussion and summary

In the following, we will contrast our findings with previous results. As for tracer diffusion, there are experimental and numerical studies in quasi-2D, which can be used for comparison. One should keep in mind, however, that our simulations have been conducted in an ideal 2D system and not in quasi-2D. Further, to our knowledge, there are no previous studies on the influence of HIs on collective diffusion of colloidal systems in neither ideal or quasi-2D systems.

In reference [6], the authors studied by digital videomicroscopy monolayers of paramagnetic polystyrene spheres confined to an air/water interface. The interactions were $\sim 1/r^3$ and therefore of relatively long range. The authors compared their experimental data with results from quasi-2D computer simulations, where hydrodynamic interactions were neglected. It seems that for the low volume

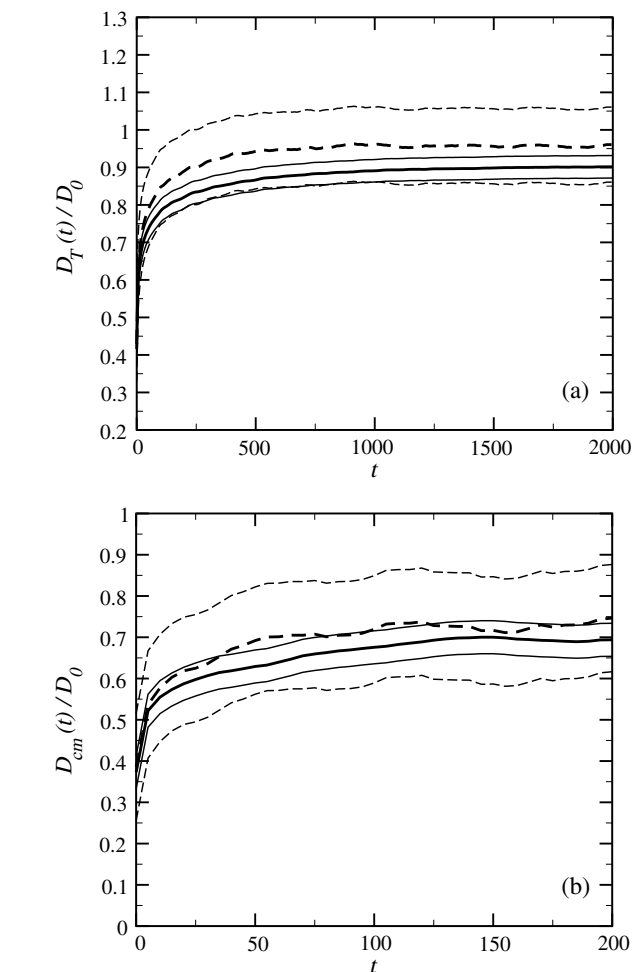


Fig. 3. (a) Scaled tracer diffusion coefficients $D_T(t)/D_0$ as functions of time for $\rho = 0.0616$ and $Sc \approx 1$. The thick dashed line is the scaled tracer diffusion coefficient computed with explicit solvent-colloid interactions, and the thin dashed lines illustrate the corresponding errors. The thick solid line is the scaled tracer diffusion coefficient obtained from simulations where the conventional solvent-colloid interactions have been replaced by multi-particle collisions. The thin solid lines represent the errors in this case. (b) Scaled CM mobilities $D_{cm}(t)/D_0$ as functions of time for $\rho = 0.0616$ and $Sc \approx 1$. The dashed and solid lines have been chosen as in part (a).

fractions ($\rho < 0.1$) studied, the scaled tracer diffusion coefficients from simulations without HIs were smaller than those obtained from experiments, in accord with our results. Additionally, the values of the scaled tracer diffusion coefficients increased with the density of colloids, which is opposed to what we see in our case. However, one should keep in mind that reference [6] focused on the low-concentration limit, while our purpose was to examine the impact of HIs on both tracer and collective diffusion over a wide concentration range, and to investigate the differences between tracer and collective diffusion. It seems obvious that at large concentrations the scaled diffusion coefficients would decrease with the density of colloids, thus the conclusions made in reference [6] are subject to

the low-density limit considered therein. Nevertheless, the main conclusion presented in reference [6] was that hydrodynamic interactions might enhance diffusion for colloids with long-range potentials. The study was complemented by reference [7], where the authors discuss their Brownian dynamics simulations, where hydrodynamic interactions had been included. They found very good agreement with the earlier experimental results.

Pesché *et al.* [8] performed quasi-2D Stokesian dynamics simulations to probe the static and dynamic properties of a monolayer of colloidal particles between two parallel walls. For hard spheres and moderately charged particles interacting with Yukawa-like potentials, they noted a modest reduction of tracer diffusion due to hydrodynamic interactions. For strongly repelling charged particles, they observed a minor enhancement of tracer diffusion. In this study, the scaled tracer diffusion coefficients seem to decrease monotonically as a function of colloidal density.

Our data indicate that in ideal 2D situations for *short-range* interactions of the form $V(r) \sim 1/r^{12}$, the HIs have a small, enhancing effect on tracer diffusion. In addition, it is clear that in our case the values of effective scaled tracer diffusion coefficients decrease monotonically with an increasing colloidal density.

Our results are in reasonably good agreement with previous studies in cases where a comparison is appropriate. Nevertheless, there remains a number of questions about the influence of HIs on tracer diffusion. Perhaps the most pressing ones are related to the nature of diffusion in 2D systems. Does the tracer diffusion studied in experiments essentially correspond to the ideal 2D situation, or is it indeed crucial to resort to a quasi-2D description? In other words, how similar are the dynamic properties of ideal and quasi-2D systems? If there are major differences, is there a crossover from the ideal 2D to the quasi-2D case, followed by another crossover to the 3D behaviour in bulk? And finally, how is the quasi-2D system then related to the two limits? Numerical simulations that probe these issues, although challenging, should be feasible in the near future. Another important direction is to systematically investigate the role of interactions. It would be interesting to study what effect softer interactions between the colloidal particles might have on the behaviour of tracer diffusion with and without hydrodynamics. Work in this direction is in progress.

As one of our main objectives has been to study the effect of HIs on collective diffusion, it is rather unfortunate that there are no experimental studies available for comparison. Thus, we are bound to summarise our findings and discuss their relevance.

We have found that when HIs are included, collective diffusion is notably different from tracer diffusion. Further, collective diffusion with HIs is utterly unlike collective diffusion in the dissipative case. These differences can be attributed to the interplay of the steeply descending mobility factor D_{cm} and the monotonously increasing thermodynamic factor ξ . The end result is a minimum or plateau of the scaled collective-diffusion coefficient at intermediate colloid concentrations.

The competition between dynamic and thermodynamic effects is an essential feature of concerted diffusion processes characterised by the collective-diffusion coefficient. Hence we feel that the behaviour found here for collective diffusion is of generic nature. It would be interesting to study how our results are affected when proceeding from an ideal 2D system to a confined 3D geometry, or how effective interactions obtained from experiments [5] are manifested in collective diffusion. Experiments, in particular, would be illuminating.

To summarise, we have presented a detailed numerical study of the effects of hydrodynamics on both self- and collective diffusion of 2D repulsive colloidal particles. This has been achieved by using a novel hybrid mesoscopic scheme for two-component liquids. We have found that the effective tracer diffusion coefficient appears to be for our choice of colloidal interactions slightly enhanced when the Schmidt number is increased, but it is not significantly altered by HIs. The collective-diffusion coefficient, however, is strongly coupled to hydrodynamics, and is distinctly different from the behaviour predicted by approaches where hydrodynamic interactions are not taken into account.

This work has been supported in part by the Academy of Finland grant No. 80246 (I.V.), through its Center of Excellence Program, and the National Graduate School in Materials Physics (E.F.). Computing resources provided by the Finnish IT Center for Sciences and the DCSC Center in Odense are gratefully acknowledged.

References

1. G. Nägele, Phys. Rep. **272**, 215 (1996).
2. C. Bechinger, Curr. Opin. Colloid Interface Sci. **7**, 204 (2002).
3. D. Frenkel, Physica A **313**, 1 (2002).
4. H. Acuña-Campa, M.D. Carbajal-Tinoco, J.L. Arauz-Lara, M. Medina-Noyola, Phys. Rev. Lett. **80**, 5802 (1998).
5. M. Brunner, C. Bechinger, W. Strepp, V. Lobaskin, H.H. Grünberg, Europhys. Lett. **58**, 926 (2002).
6. K. Zahn, J.M. Méndez-Alcaraz, G. Maret, Phys. Rev. Lett. **79**, 175 (1997).
7. B. Rinn, K. Zahn, P. Maass, G. Maret, Europhys. Lett. **46**, 537 (1999).
8. P. Pesché, G. Nägele, Phys. Rev. E **62**, 5432 (2000).
9. P. Pesché, M. Kollmann, G. Nägele, J. Chem. Phys. **114**, 8701 (2001).
10. M. Kollmann, R. Hund, B. Rinn, G. Nägele, K. Zahn, H. König, G. Maret, R. Klein, J.K.G. Dhont, Europhys. Lett. **58**, 919 (2002).
11. H. Löwen, Phys. Rev. E **53**, R29 (1996).
12. J.M. Lahtinen, T. Hjelt, T. Ala-Nissila, Z. Chvoj, Phys. Rev. E **64**, 021204 (2001).
13. W. Hess, R. Klein, Adv. Phys. **32**, 173 (1983).
14. A.V. Indrani, S. Ramaswamy, Phys. Rev. Lett. **74**, 1491 (1995).
15. H. Aranda-Espinoza, M. Carbajal-Tinoco, E. Urrutia-Banuelo, J.L. Arauz-Lara, J. Alejandre, J. Chem. Phys. **101**, 10925 (1994).

16. H. Acuña-Campa, M. Medina-Noyola, *J. Chem. Phys.* **113**, 869 (2000).
17. A. Malevanets, R. Kapral, *J. Chem. Phys.* **110**, 8605 (1999).
18. A. Malevanets, R. Kapral, *J. Chem. Phys.* **112**, 7260 (2000).
19. A. Malevanets, J.M. Yeomans, *Europhys. Lett.* **52**, 231 (2000).
20. R.D. Groot, P.B. Warren, *J. Chem. Phys.* **107**, 4423 (1997).
21. C.P. Lowe, *Europhys. Lett.* **47**, 145 (1999).
22. E. Falck, O. Punkkinen, I. Vattulainen, T. Ala-Nissila, *Phys. Rev. E* **68**, 050102 (2003).
23. S.H. Lee, R. Kapral, *Physica A* **298**, 56 (2001).
24. A. Lamura, G. Gompper, T. Ihle, D.M. Kroll, *Europhys. Lett.* **56**, 319 (2001).
25. A. Malevanets, J.M. Yeomans, *Comput. Phys. Commun.* **129**, 282 (2000).
26. N. Kikuchi, A. Gent, J.M. Yeomans, *Eur. Phys. J. E* **9**, 63 (2002).
27. A. Lamura, G. Gompper *Eur. Phys. J. E* **9**, 477 (2002).
28. T. Ihle, D.M. Kroll, *Phys. Rev. E* **63**, 020201 (2001).
29. T. Ihle, D.M. Kroll, *Phys. Rev. E* **67**, 066705; 066706 (2003).
30. N. Kikuchi, C.M. Pooley, J.F. Ryder, J.M. Yeomans, *J. Chem. Phys.* **119**, 6388 (2003).
31. S.C. Ying, I. Vattulainen, J. Merikoski, T. Hjelt, T. Ala-Nissila, *Phys. Rev. B* **58**, 2170 (1998).
32. T. Hjelt, I. Vattulainen, T. Ala-Nissila, S.C. Ying, *Surf. Sci.* **449**, L255 (2000).
33. B.J. Alder, T.E. Wainwright, *Phys. Rev. A* **1**, 18 (1970).
34. M.A. van der Hoef, D. Frenkel, A.J.C. Ladd, *Phys. Rev. Lett.* **67**, 3459 (1991).
35. J.R. Dorfman, E.G.D. Cohen, *Phys. Rev. A* **7**, 776 (1972).
36. M.H. Ernst, E.H. Hauge, J.M.J. van Leeuwen, *Phys. Rev. A* **4**, 2055 (1971).
37. C.P. Lowe, D. Frenkel, *Physica A* **220**, 251 (1998).
38. M. Medina-Noyola, *Phys. Rev. Lett.* **60**, 2705 (1988).
39. R. Gomer, *Rep. Prog. Phys.* **53**, 917 (1990).
40. T. Boublik, *Mol. Phys.* **29**, 421 (1975).
41. Z. Chvoj, private communication, unpublished (2003).